

Article

# The Albitization of K-Feldspar in Organic- and Silt-Rich Fine-Grained Rocks of the Lower Cambrian Qiongzhusi Formation in the Southwestern Upper Yangtze Region, China

Huajun Min <sup>1,2,3</sup> , Tingshan Zhang <sup>3,\*</sup>, Yong Li <sup>1,2,\*</sup>, Shaoze Zhao <sup>2</sup>, Jilin Li <sup>3</sup>, Dan Lin <sup>4,5</sup> and Jincheng Wang <sup>6</sup>

<sup>1</sup> State Key Laboratory of Oil and Gas Reservoir Geology and Exploitation, Chengdu University of Technology, Chengdu 610059, China; minesky@126.com

<sup>2</sup> College of Energy Resources, Chengdu University of Technology, Chengdu 610059, China; zszcdut@126.com

<sup>3</sup> School of Geoscience and Technology, Southwest Petroleum University, Chengdu 610500, China; ljlgeology@163.com

<sup>4</sup> Shale Gas Evaluation and Exploitation Key Laboratory of Sichuan Province, Chengdu 610091, China; lindan332000@126.com

<sup>5</sup> Sichuan Keyuan Testing Centre of Engineering Technology, Chengdu 610091, China

<sup>6</sup> PetroChina Dagang Oilfield Company, Tianjin 300280, China; wangjcheng@petrochina.com.cn

\* Correspondence: zts\_3@126.com (T.Z.); liy@cdut.edu.cn (Y.L.)

Received: 23 September 2019; Accepted: 3 October 2019; Published: 8 October 2019



**Abstract:** The albitization of K-feldspar is a common diagenetic process that has thus far received little attention and is not fully understood in fine-grained sedimentary rocks. To better understand the albitization of K-feldspar, studies in organic- and silt-rich fine-grained rocks of the lower Cambrian Qiongzhusi Formation in the southwestern Upper Yangtze region, China, were carried out via X-ray diffractometry (XRD) and field emission scanning electron microscopy (FE-SEM). The results show that five types of albitized K-feldspar textures have developed: microcrystal albite replacement, irregular blocky replacement along margins, cleavage planes or microcracks of K-feldspars, complete pseudomorphic replacement, albite overgrowth, and albite pore filling. Organic- and silt-rich fine-grained rocks differ from sandstones and mudstones in terms of the rock structure and mineral assemblage, which results in differences in the textures and degree of albitization of K-feldspar. Illitization of clay has an impact on the albitization of K-feldspar. In provenance analyses using feldspar, fine-grained rocks, especially those that underwent mesogenesis, should be treated with caution because detrital feldspars have been destroyed. Theoretically, the albitization of K-feldspar could increase the porosity of reservoirs, although, from our observations, most of the related secondary pores are cancelled out or became isolated pores due to other diagenetic processes (compaction, cementation, etc.) in organic- and silt-rich fine-grained rocks.

**Keywords:** albitization of K-feldspar; diagenesis; fine-grained rocks; Qiongzhusi formation

## 1. Introduction

Fine-grained rocks, which are predominantly composed of materials <62.5  $\mu\text{m}$ , including siltstone (grain sizes from 62.5 to 4  $\mu\text{m}$ ) and mudstone (grain sizes <4  $\mu\text{m}$ ), have the highest proportion in sedimentary rocks [1]. However, studies on diagenesis in fine-grained rock are relatively scarce. Recently, due to the global upsurge in shale gas exploration and development, the diagenesis of fine-grained rocks has received renewed attention [2–6]. Diagenesis usually has significant impacts on

the properties of shales [2,4,7], especially for the growth of diagenetic authigenic quartz, which can facilitate increases in the brittleness and strength of shales [4,7,8] and thus affect the hydrofracturing of shales and the development of shale gas. Therefore, more attention has been paid to diagenetic authigenic quartz in fine-grained rocks [2,4,5,7]. The albitization of K-feldspar is a diagenetic process in which K-feldspar loses K and gains Na simultaneously, and hence converts to albite [9–11]. The albitization of K-feldspar in sandstones has been extensively studied [9,10,12,13]. Although many researchers have noticed this diagenetic process in fine-grained rocks [2,3,6,14,15], very little work has been done [14,15]. Moreover, the albitization of K-feldspar in fine-grained rocks has not been fully understood. K-feldspar albitization is a diagenetic process that can significantly alter the original mineral assemblage; it impacts other diagenesis processes (such as clay mineral illitization), and results in the cementation of fine-grained rocks [14–16]. Thus, studying the albitization of K-feldspar in fine-grained rocks is of great relevance.

Many studies carried out on the albitization of K-feldspar in sandstones have shown that (1) the albitization of K-feldspar proceeds by a dissolution-precipitation mechanism [10,17]. (2) The main textures of albitized K-feldspar are albitization along the cleavages, microfractures, and margins of grains, albite overgrowth, and complete replacement and pore-filling albite [9,10,12]. (3) The sources of Na for albitization are pore water, brine related to evaporite rocks, and clay mineral transformation [10,17,18]. (4) The factors affecting the albitization of K-feldspar are temperature, rock permeability,  $\text{Na}^+/\text{K}^+$ , parent mineral surface dissolution kinetics, etc. [10]. Few studies have been performed on the albitization of K-feldspar in fine-grained rocks. Milliken (1992) found that in Frio mudrocks, as in sandstones, the albitization of K-feldspar proceeds through a dissolution-precipitation mechanism, with the K-feldspar composition changing more slowly with depth than in adjacent sandstones, and that intragranular pores in feldspars are scarce in Frio mudrocks [14]. Approximately 56–68% of K-feldspar has been albitized in Frio mudrocks [10] (calculated from Table 1 in Milliken [14], which assumes that the provenance has not changed greatly for all samples). Lee and Lee (1998) found that K-feldspar is only partially albitized to unalbitized in non-marine mudrocks of the Sindong and Hayang groups [15].

The feldspar content in organic- and silt-rich fine-grained rocks of the Qiongzhusi Formation in the study area is relatively high (generally more than 15%), and the albitization of K-feldspar is a common and strong diagenetic process. Therefore, the Qiongzhusi Formation is an ideal subject for our study. To better understand the albitization of K-feldspar in fine-grained rocks, studies were carried out via X-ray diffractometry (XRD) and field emission scanning electron microscopy (FE-SEM). The organic- and silt-rich fine-grained rocks of the Qiongzhusi Formation are potential shale gas reservoirs in Paleozoic formations in South China, where industrial gas flow has been obtained [19]. However, very little work has been conducted on the diagenesis of the Qiongzhusi Formation. Our study can also provide support for investigating the shale gas geology of the Qiongzhusi Formation in the study area. In this study, five types of albitized K-feldspar textures are identified, some of which have not been previously reported. We found that the illitization of clay minerals, rock structure, and mineral assemblage of rocks may also have an impact on the K-feldspar albitization process. No secondary pores related to the albitization of K-feldspar were identified, but the albitization process may also promote improvements in the brittleness and the quality of fine-grained rocks as a shale gas reservoir.

**Table 1.** XRD mineral assemblage and TOC of the Qiongzhusi Formation samples in the study area.

Well/Section	Sample ID	Mineral Contents (%)							Clay Mineral Contents (%)						TOC (%)
		Quartz	K-Feldspar	Plagioclase	Calcite	Dolomite	Pyrite	Clay Minerals	K	C	I	S	I/S	C/S	
Majinzi	Majinzi-1*	59.6	2.4	17.0	0.0	0.0	0.0	20.5	1	1	38	0	52	8	2.7
Majinzi	Majinzi-2*	50.3	7.0	14.3	0.0	0.0	0.0	25.5	0	0	38	0	62	0	3.6
Majinzi	Majinzi-3	48.0	3.4	17.9	0.0	1.1	0.0	24.6	0	0	26	0	74	0	2.5
Majinzi	Majinzi-4	48.2	4.8	17.1	0.0	0.0	0.0	26.0	0	3	20	0	77	0	2.4
Majinzi	Majinzi-5	44.9	3.4	19.4	0.4	0.8	0.0	24.5	0	0	27	0	70	3	2.0
Majinzi	Majinzi-6	41.2	2.2	19.6	0.0	2.0	0.0	28.6	0	3	31	0	66	0	0.5
Majinzi	Majinzi-7*	41.4	3.3	18.4	0.0	2.9	0.0	25.4	0	20	30	0	41	9	1.6
Majinzi	Majinzi-8	40.3	3.5	23.0	0.5	1.1	0.0	29.3	0	38	18	0	26	18	0.2
Majinzi	Majinzi-9	51.7	3.7	25.7	7.0	1.0	1.2	9.7	0	39	23	0	16	22	0.6
Majinzi	Majinzi-10	40.2	6.0	19.2	0.0	0.0	0.0	23.8	0	4	28	0	52	16	0.5
Majinzi	Majinzi-11*	47.0	6.6	20.2	0.0	0.0	0.0	23.8	0	14	34	0	42	10	2.5
Majinzi	Majinzi-12	46.5	2.9	10.9	0.0	0.0	0.0	33.2	0	2	26	0	69	3	3.0
Z1	Z1-1	73.3	1.5	3.0	9.4	0.6	1.6	9.8	0	0	24	0	76	0	6.6
Z1	Z1-2*	51.3	1.2	9.7	4.6	4.3	5.9	20.6	3	0	37	0	60	0	4.8
Z1	Z1-3	35.5	1.8	14.4	2.4	3.2	6.7	36.0	1	1	25	0	73	0	2.6
Z1	Z1-4	32.7	1.8	8.0	2.3	7.2	9.1	37.0	0	3	32	0	61	4	2.6
Z1	Z1-5*	37.0	1.8	13.6	0.4	5.7	8.9	31.8	1	2	13	0	84	0	3.0
Z1	Z1-6	39.2	2.4	19.1	5.2	5.4	9.4	19.3	0	10	17	0	61	12	4.2
Z1	Z1-7	37.7	3.0	18.9	3.5	1.2	4.6	28.4	0	6	21	0	68	5	3.1
Z1	Z1-8	32	2.1	17.0	2.6	8.9	13.9	21.8	0	8	23	0	63	6	3.0
Z1	Z1-9*	36.3	2.3	18.9	4.5	2.4	4.7	30.9	0	22	24	0	43	11	1.8
Z1	Z1-10	44.5	2.7	21.0	1.5	0.0	3.3	27.0	0	13	19	0	59	9	1.8
Z1	Z1-11	38.3	2.4	18.7	0.9	2.6	3.3	32.7	0	8	30	0	55	7	1.9
Z1	Z1-12	36.8	3.1	20.8	2.0	0.2	1.5	32.3	1	7	14	0	67	11	1.8
Z1	Z1-13	43.0	3.9	22.1	3.8	0.0	2.1	22.1	3	9	19	0	52	17	1.9
Z1	Z1-14	35.4	3.2	20.3	3.5	0.0	1.2	32.4	0	35	22	0	29	14	1.7
Z1	Z1-15*	37.2	3.3	20.0	3.9	0.0	2.5	31.2	0	34	12	0	42	12	1.7
Z1	Z1-16	38.3	3.6	22.4	3.9	0.0	2.4	29.4	0	31	13	0	41	15	1.3
Z1	Z1-17	38.7	2.8	24.2	3.9	0.0	1.5	24.8	0	28	15	0	45	12	1.3
Z1	Z1-18*	37.8	2.6	23.0	3.4	0.8	1.4	29.5	0	39	22	0	36	3	1.1
Z1	Z1-19	41.7	3.7	28.3	10.1	0.0	1.1	12.2	0	38	12	0	31	19	1.1
Z1	Z1-20	45.2	4.4	21.4	4.1	0.0	0.0	23.0	0	48	9	0	29	14	0.9
Z1	Z1-21	39.1	3.1	24.7	6.9	0.6	1.0	21.3	0	42	12	0	29	17	1.2
Z1	Z1-22	42.0	2.9	28.0	9.0	0.0	3.3	14.0	0	45	10	0	28	17	0.8
Z1	Z1-23	41.4	2.4	26.8	6.5	0.6	1.2	17.6	0	42	14	0	22	22	1.0
Z1	Z1-24	37.8	2.2	27.4	4.3	0.6	1.2	21.9	0	44	14	0	24	18	1.2
Range value		32–73.3	1.2–7	3–28.3	0–10.1	0–8.9	0–13.9	9.8–37	0–3	0–48	9–38	0	16–84	0–22	0.2–6.6
Average value		42.5	3.2	19.3	3.1	1.5	2.6	25.1	0.3	17.8	22.0	0	50.7	9.3	2.1

<sup>1</sup> K= kaolinite, C = chlorite, I = illite, S = smectite, I/S = illite/smectite mixed-layer mineral, C/S = chlorite/smectite mixed-layer mineral. <sup>2</sup> Majinzi-1\* = FE-SEM sample.

## 2. Geological Setting

The study area is located at the intersection of Sichuan, Yunnan, and Guizhou provinces in southwestern China and belongs to the southwestern margin of the Yangtze Plate (Figure 1). The Qiongzhusi Formation, which is one of the important source rocks in South China, belongs to the lower Cambrian [20–22] and includes some layers rich in Ni, Mo, V, and other rare metals [23]. The Qiongzhusi Formation, with a regional unconformity at the bottom, was deposited during a large-scale transgression [24], and organic- and silt-rich fine-grained rocks were deposited mainly in the lower part of the formation in the study area. During the deposition of the Qiongzhusi Formation, most of the Upper Yangtze area was flooded by seawater except for the West Sichuan-Central Yunnan Oldland (in the western part of Figure 1) [25], and the water depth increased on the whole from west to east. A coastal shelf basin sedimentary system correspondingly developed from west to east in the Upper Yangtze region (Figure 1) during deposition. The sandstones, sandy shales, pelitic siltstones, carbonaceous shale, siliceous shale, etc. were deposited successively in response to the increasing water depth from west to east [23,26]. During the deposition of the Qiongzhusi Formation, the study area was located in the shallow shelf, and fine-grained rocks rich in organic matter and silt were deposited in the early stage. The burial history shows that before the Silurian, the southwestern Yangtze margin subsided stably and that the Qiongzhusi Formation was buried to a maximum depth of 3000–4000 m [27]. From the Devonian to the Carboniferous, the southwestern Yangtze margin was relatively stable and the burial depth of the Qiongzhusi Formation changed little [27]. From the Permian to the Jurassic, the southwestern Yangtze margin subsided stably, and the Qiongzhusi Formation was buried with a maximum depth of more than 6000 m and a maximum geothermal temperature of more than 200 °C [27]. Therefore, the Qiongzhusi Formation has undergone mesogenesis processes. Since the Cretaceous, under regional tectonic compression, the crust in the study area gradually rose, which resulted in an increasingly shallow burial depth of the Qiongzhusi Formation [27] and the exposure of the Qiongzhusi Formation at the surface in some areas.

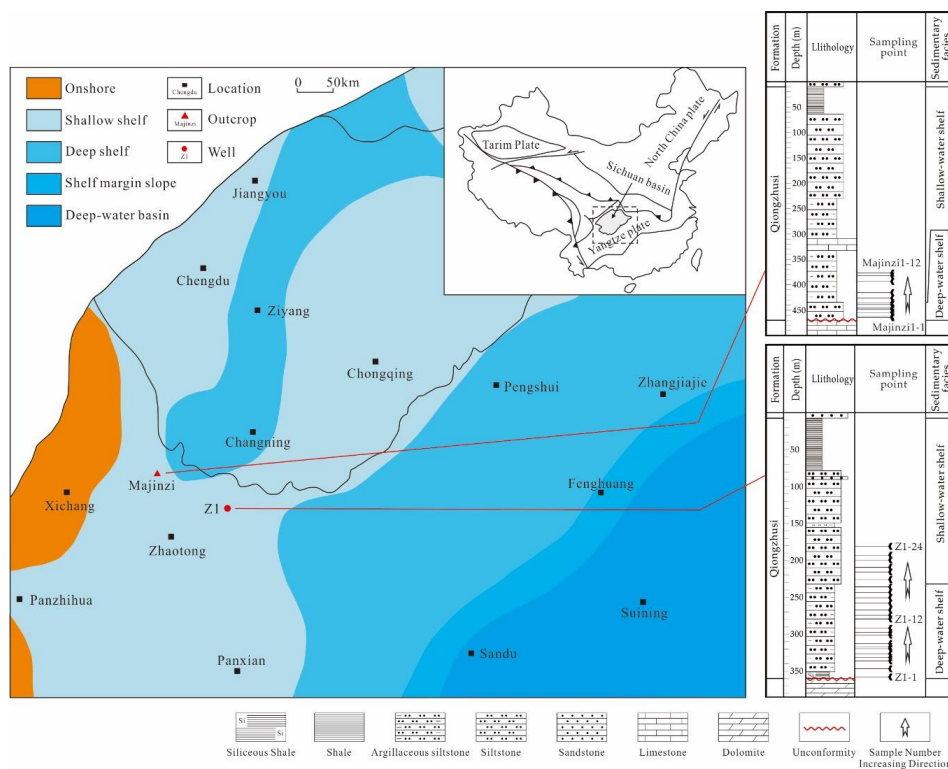


**Figure 1.** Sedimentary facies distribution map of the lower Cambrian Qiongzhusi Formation in the Upper Yangtze area (modified from [25]).

### 3. Samples and Methods

Samples of organic- and silt-rich fine-grained rocks were taken from an outcrop in Majinzi Township, Leibo County, Sichuan Province, and from well Z1, Liaoyeba Village, Yanyuan Township, Zhenxiang County, Yunnan Province (Figure 1). The fresh samples were divided into several smaller blocks to test the whole-rock mineralogy, clay mineral assemblage, and total organic carbon content (TOC). Some of the samples were selected to observe via FE-SEM.

The whole-rock mineralogy and clay mineral assemblage were determined by XRD using a D8 Advance instrument with a Cu anticathode (40 kV; 40 mA) at the Shale Gas Evaluation and Exploitation Key Laboratory of Sichuan Province, China. In total, 36 samples were analyzed (Table 1, Figure 1). Each sample (1–2 g) for whole-rock mineralogy testing was first dried at temperatures below 60 °C and then crushed to a size of less than 75 µm. Powdered whole-rock samples were scanned over an angular range of 3–45° ( $2\theta$ ) at a rate of one degree/minute. The percentages of minerals in each sample were calculated using the area of the principle peaks of each mineral with correction for Lorentz polarization [28]. Samples for clay mineral assemblage testing were first crushed to less than 1 mm in diameter and then soaked in distilled water and dispersed by ultrasound. Then, the <2 µm fraction (suspension) was extracted for testing. To solve peak overlap issues, clay-fraction analysis was performed with multiple treatments: air-dried, ethylene glycol (60 °C for more than 8 h), and heated (450–550 °C for 2.5 h). The air-dried clay-fraction mounts and heated clay-fraction mounts were scanned over an angular range of 2.5–15° ( $2\theta$ ) at 1.5°/minute. The glycol-solvated clay fraction was scanned over an angular range of 2.5–30° ( $2\theta$ ) at 1.5°/minute. Different clay minerals were estimated by the subtraction method with peak areas in the diffractograms of air-dried, ethylene-glycol, and heated mounts. Detailed information about sample preparation, analysis, and interpretation refers to the methods provided by the China National Energy Administration [29].

The TOC of 36 samples from the outcrop located in Majinzi and from well Z1 (Table 1) was determined by the combustion method using a Leco CS230 carbon analyzer at the State Key Laboratory of Oil and Gas Reservoir Geology and Exploitation, China. The inorganic carbon was first removed with hydrochloric acid, and the samples were then rinsed repeatedly with distilled water. Next, the samples were heated in an oxygen-filled pyrolysis furnace (~1500 °C), and carbon dioxide was measured with an infrared detector. Measurements were calibrated using carbon standards.

The FE-SEM samples were polished by Ar ion beam milling and then coated with platinum (Pt) to increase conductivity before observation via FE-SEM. The polished thin sections were examined by FE-SEM using a FEI Quanta 650 apparatus. Back-scattered electron images were taken along with the energy-dispersive X-ray spectroscopy (EDS) to determine the textures of albitized K-feldspar. Sample polishing was completed for nine samples using a GATAN PECS II 685 instrument. The FEI Quanta 650 FEG microscope provided high spatial resolution (~1 nm at 30 kV). The polishing and FE-SEM examination were completed at the State Key Laboratory of Oil and Gas Reservoir Geology and Exploitation, China.

## 4. Results

### 4.1. Mineral Assemblage

The results show that the Qiongzhusi Formation in the study area is rich in organic matter and silt, and the rock is mainly supported by silt-sized detrital grains (Figure 2). XRD analysis shows that the minerals are mainly composed of quartz (ranging from 32.7% to 73.3%), clays (ranging from 9.7% to 37%), plagioclase (ranging from 3% to 28.3%; calcium-bearing plagioclase was not found in our test by EDS, which may indicate that all or most of the plagioclase has been albitized because of its thermodynamic instability [9]), carbonate minerals (including calcite and dolomite, ranging from 0% to 10.6%), K-feldspar (ranging from 1.2% to 7%), and pyrite (ranging from 0% to 13.9%) (Table 1, Figure 3). Clay minerals are composed of illite, illite/montmorillonite mixed-layer minerals, chlorite, and chlorite/montmorillonite mixed-layer minerals (Table 1, Figure 3). Some samples contain a small

amount of kaolinite (Table 1, Figure 3). The TOC of the samples ranges from 0.2% to 6.6%, with an average of 2.1% (Table 1).



**Figure 2.** Photographs of organic- and silt-rich fine-grained rocks of the Qiongzhusi Formation in the study area. (a,b) Photographs of outcrops; (c) photograph of a core; (d) thin section photomicrograph; (e) SEM photomicrograph.

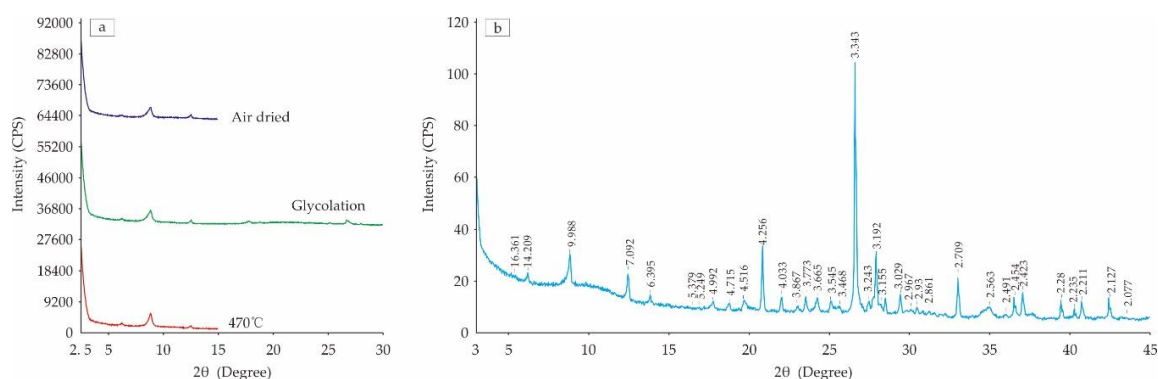


**Figure 3.** Representative XRD spectra of the clay fraction (a) and bulk rock (b) (sample Z1-8).

#### 4.2. General Diagenesis

The most common diagenetic authigenic minerals in the Qiongzhusi Formation samples, as determined by EDS and backscattered imaging, include quartz, illite, illite/smectite mixed-layer

mineral, chlorite, chlorite/smectite mixed-layer mineral, albite, pyrite, calcite, and apatite (Figure 4). Authigenic quartz usually fills the intergranular pores with numerous microcrystals (Figure 4b,c) or overgrows around detrital quartz (Figure 4b). Authigenic albite can be seen as microcrystal albite replacement, irregular blocky replacement along the margins, cleavage planes or microcracks of K-feldspar grains, complete replacement (pseudomorphic replacement), albite overgrowth, and albite cementation in pores (discussed in detail in the following sections). Pyrite occurs in the form of framboidal pyrite (Figure 4d), pyrite crystals filled in matrix pores or engulfed in quartz, feldspar and muscovite (Figure 4b,e), and anhedral pyrite (Figures 5d–h and 6). Calcite mainly fills the pores as cement (Figure 4f) or replaces other minerals, such as quartz, and is common in samples of well Z1. Samples from Majinzi contain very little or no calcite (Table 1). Apatite includes strawberry-like apatite and euhedral apatite crystals. Strawberry-like apatite fills in the intergranular pores and euhedral apatite crystals are engulfed in albite crystals (Figures 5g and 6). In addition, limonite can be also found between the grains or in the space between the grain and matrix and in albite intragranular pores (Figures 5h and 6) in the samples of Majinzi.

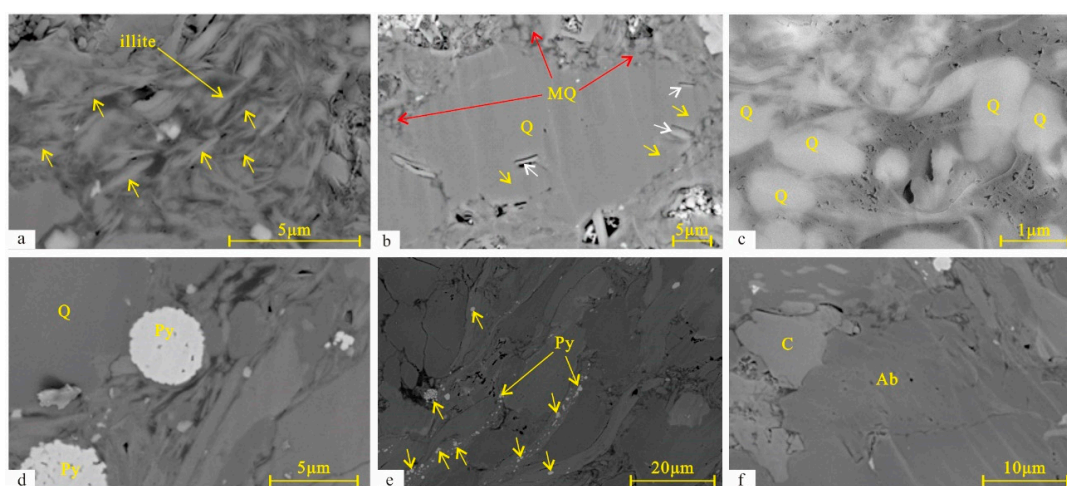


**Figure 4.** Diagenetic minerals in organic- and silt-rich fine-grained rocks of the Qiongzhusi Formation. (a) Clay minerals in matrix, where most of the clay minerals are illite; (b) quartz overgrowth (yellow arrow), where unknown minerals (white arrow) were engulfed because of the overgrowth and numerous microcrystalline quartz (MQ) can be also seen; (c) authigenic microcrystalline quartz in matrix; (d,e) strawberry-like and monocrystalline pyrite crystals; and (f) calcite cement in an intergranular pore. Q = quartz, MQ = microcrystalline quartz, C = calcite, Py = pyrite, Ab = albite.

Illite, illite/smectite mixed-layer mineral, chlorite, and chlorite/smectite mixed-layer mineral are mainly the products of montmorillonite transformation due to the increasing temperature with burial [16,30]. Some illite may also be formed by kaolinite illitization at temperatures exceeding 120–130 °C (discussed below) [31,32]. The possible sources of silica for authigenic quartz reported in sedimentary rocks are mainly the smectite to illite transition, pressure dissolution of detrital quartz, biogenic silica, and alteration of volcanic glass [33] (and references therein). In this paper, the exact sources of silica and their corresponding contributions cannot be determined. However, the volcanic glass source can be excluded because no volcanic eruptions were reported in the study area during the deposition of the Qiongzhusi Formation. In addition, the characteristics of numerous microcrystalline quartzes in the intergranular pores are very similar to those in Longmaxi Formation shale, which has been proven to come from biological silicon [34]. Framboidal pyrite is generally considered to be formed at the syngenetic stage and usually found in an anoxic sedimentary environment [35,36]. According to the positional relationship between diagenetic minerals (Figure 5g,h), pyrite crystals should be formed before the albitization of feldspar, or formed simultaneously with framboidal pyrite if it is deposited in a weakly oxygenated bottom water environment [37]. Calcite cements in

organic-rich mudstone successions have been widely regarded as the result of bacterial metabolic activity during the syngenetic period [5] (and references therein). Calcite can also result from albitization of plagioclase [9,14]. According to the observation of SEM images, we cannot determine whether the plagioclase albitization process took place because no plagioclase was found. However, we found a weak positive correlation in the calcite-plagioclase scatter plot (Figure 7), which may indicate that the albitization of plagioclase has taken place in the study area, or they are controlled by the same factors. The size of strawberry apatite is generally relatively larger (up to 40–50  $\mu\text{m}$ ), which indicates that strawberry apatite should be formed before intense compaction. Limonite may be formed by the oxidation of pyrite on the surface. In addition, evidence of feldspar dissolution is observed in some samples from Majinzi (Figure 5a,d). In Figure 5e–g, the euhedral apatite crystals and clay minerals in the albite grains are probably fillings of dissolution pores.

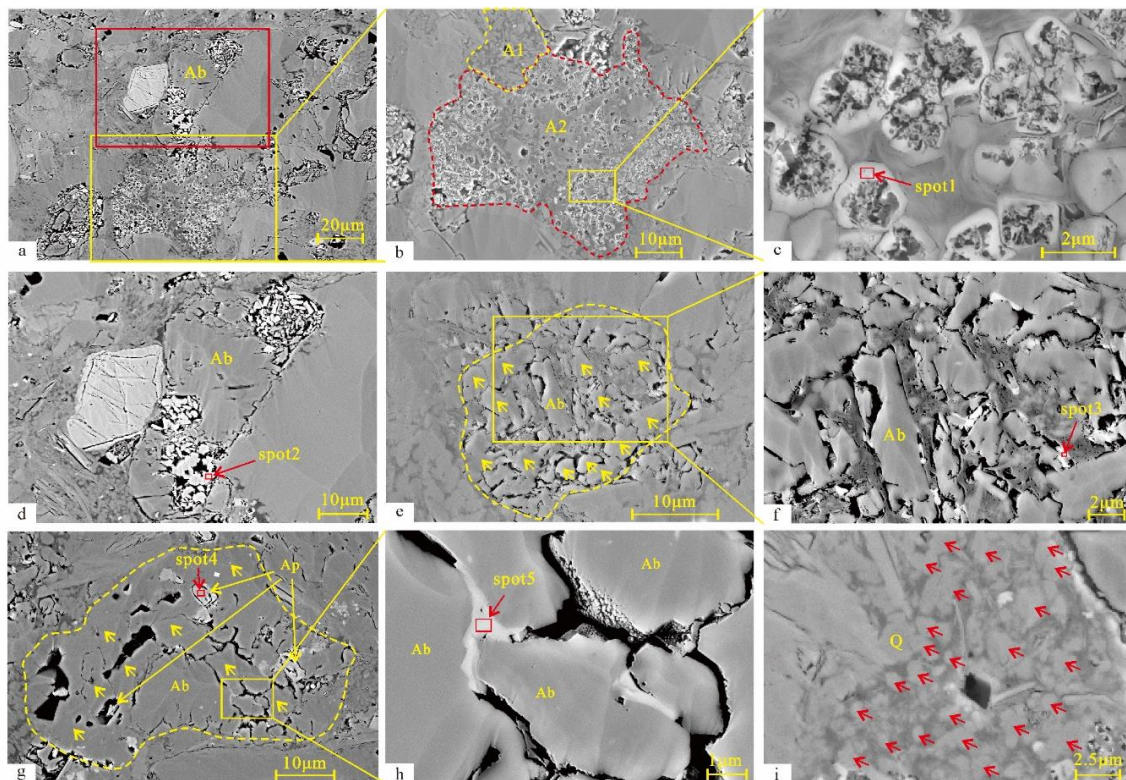


**Figure 5.** Part of the diagenesis in the Qiongzhuai Formation. (a) Dissolution pores filled with pyrite developed in a replacement albite grain (Ab) (an enlarged view shown in (d)) and strawberry-like apatite in a intergranular pore; (b) enlarged view of the yellow box in (a); microcrystalline quartz (in A1) (enlarged view shown in (j)) and strawberry-like apatite (in A2) developed in the intergranular pore; from the positional relationship between them; thus, strawberry-like apatite appears to predate the formation of microcrystalline quartz; (c) enlarged view of the yellow box in (b), where clay minerals contaminated by organic matter can be seen between the apatite crystals; (d) enlarged view of the red box in (a); (e) particle consisting of several albite crystals between which clay minerals contaminated by organic matter and mixed minerals of pyrite and limonite can be seen as shown in (f); albite crystals are small (generally less than 4  $\mu\text{m}$ ), anhedral, and some of the crystals interlock with each other; (f) enlarged view of the yellow box in (e); (g) particle consisting of several albite crystals, between which euhedral apatite crystals and anhedral pyrite developed; albite crystals are relatively coarser and part of the apatite crystals dissolved in the superficial environment, and this image shows that euhedral apatite crystals predate the formation of albite, which in turn predates the formation of anhedral pyrite; (h) enlarged view of the yellow box in (g); and (i) enlarged view of the yellow box in (a). Ab and yellow arrow = albite, Q and red arrow = quartz, Ap = apatite.

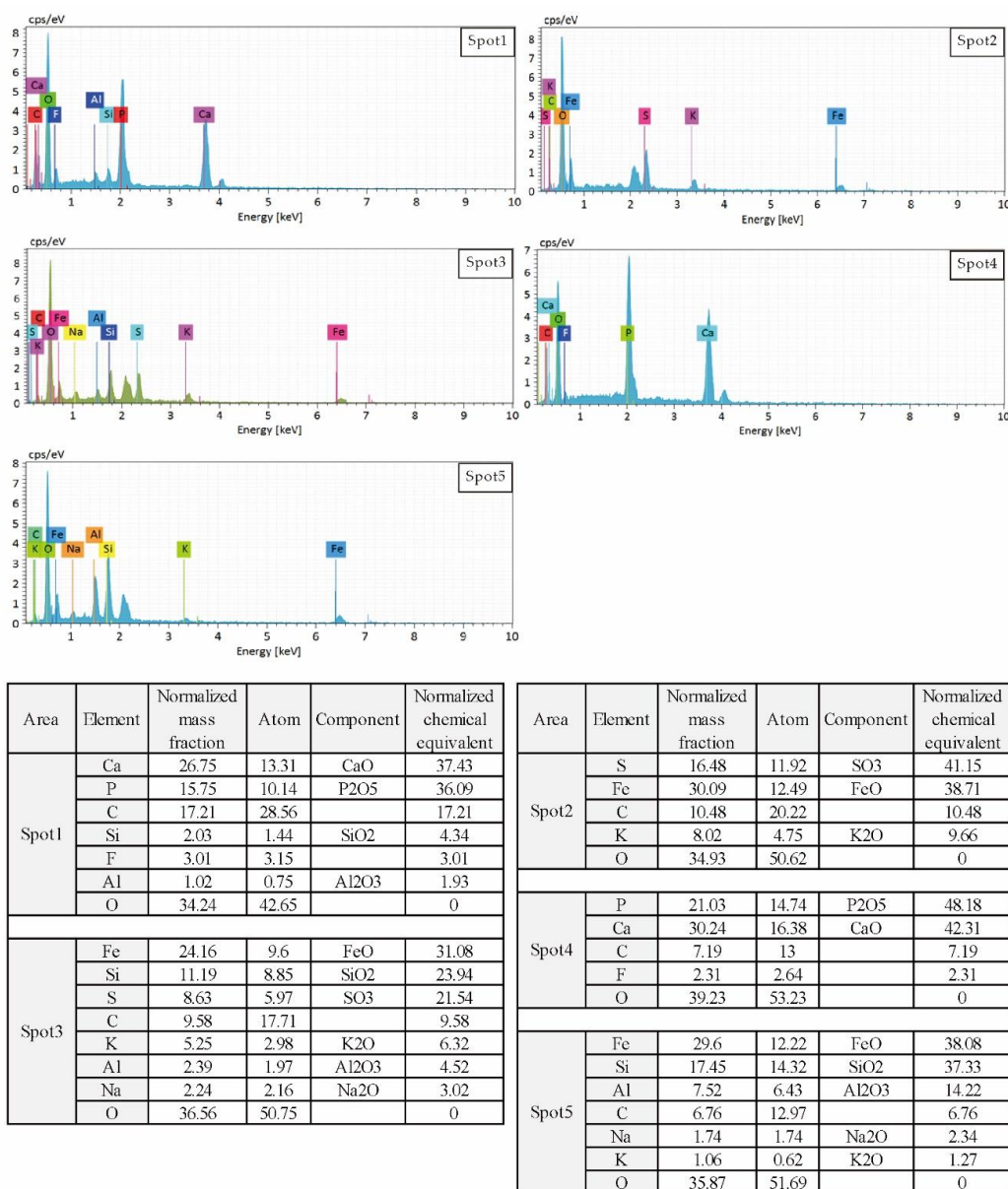


**Figure 6.** Energy spectrum and respective element composition of the detection areas marked in Figure 5. Based on the composition, morphology, and grayscale, the figure suggests that Spots 1 and 4 are apatite, Spot 2 is pyrite, Spot 3 is a mixture of pyrite and limonite, and Spot 5 is limonite.

According to previous studies [9,14,16,30–32,35–38] and the positional relationship between diagenetic minerals, the following diagenetic sequences can be established: framboidal pyrite, pyrite crystals (?), and calcite cements formed during deposition and feldspar dissolution, which likely occurred during eogenesis, predates the pore-filling anhedral pyrite (Figure 5d–h) and euhedral apatite crystals in the albite grains (Figure 5g). In addition, strawberry-like apatite occupied most of the intergranular pore in Figure 5b,i and appears to predate the formation of microcrystalline quartz, whereas in the replacement albite (Figure 5e,f), the albitization of feldspar predates anhedral pyrite, which formed before liquid hydrocarbon expulsion from kerogen (during the oil window) (Figure 5e,f). Transformations of mectite to illite and chlorite started when the formation temperature exceeded approximately 50 °C and resulted in SiO<sub>2</sub> cementation and overgrowth; transformations of kaolinite to illite or chlorite occurred when the formation temperature exceeded 120–130 °C. With depth and higher temperatures during burial, the organics in the rocks broke down to yield oil, then oil with gas and finally dry oil [38]. Maximum oil generation occurred in the oil window, during which and in

the following stage all or most of the pores were filled with oil or gas. Therefore, all the diagenesis processes in the rocks were inhibited or even stopped [39]. The temperature at which maximum oil generation starts to occur ranges from 50 °C to 130 °C, which is mainly related to the sulfur content [38]. Some samples contain a small amount of kaolinite, which may indicate that the transformations of kaolinite to illite or chlorite may be affected by the hydrocarbon charge during the oil window (resulting in incomplete transformations). The diagenetic sequence chart of the Qiongzhusi Formation is shown in Figure 8. It is noteworthy that samples from Majinzi that have undergone feldspar dissolution have a very low carbonate content or no carbonate. This coincidence is very likely to indicate that all or most of the plagioclase and Ca<sup>2+</sup> had been removed from the rocks because of dissolution. Otherwise, calcite formed during deposition (cements) or from plagioclase albitization in the subsequent diagenesis stages [9,14] would be preserved well, because the pH of pore water is buffered by feldspar rather than calcite during mesogenesis [40]. Previous studies have also suggested that, in early eogenesis, strong diagenesis processes can take place because the rocks are in an open system [41].

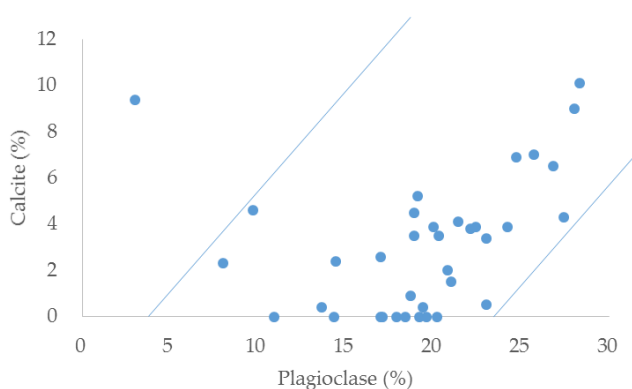


Figure 7. Calcite-plagioclase scatter plot of the Qiongzhusi Formation.

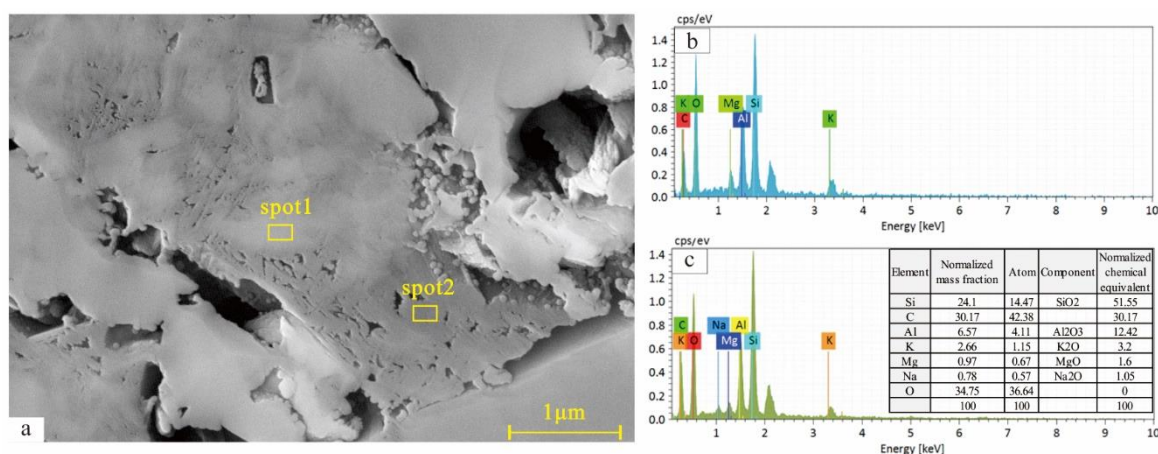
Diagenetic stage	Deposition	Berial		Uplift
	Syngensis	Early (eogenesis)	Late (mesogenesis)	(Telodiagenesis)
Framboidal pyrite and pyrite crystals cement		.....		
Calcite cement and replacement		.....		
Mechanical compaction		—————		
Feldspar dissolution		—————		
Kaonilite cementation		—————		
Strawberry-like apatite cement and apatite crystals		—————		
Quartz cement and over growth		————— (?)		
K-feldspar albitization	(?)	..... (?)		
Plagioclase albitization (?)		..... (?)		
Albite cement and overgrowth		..... (?)		
Calcite dolomitization		..... (?)		
Transformations of mectite to illite and chlorite		..... (?)		
Liquid hydrocarbon expulsion		(?) ..... (?)		
Gaseous hydrocarbon expulsion			.....	
Transformations of kaolinite to illite and chlorite			... (?)	
Limonite (Oxidation of pyrite)				—————
Apatite dissolution				—————
Pyrtie dissolution				—————

Figure 8. Diagenetic sequence chart of the Qiongzhusi Formation. The length of the solid black bars indicates the relative duration of diagenetic events. Broken lines indicate the approximate timing of diagenetic events. The question marks represent an uncertain end or start time of the diagenetic processes.

### 4.3. Texture of Albitized K-Feldspar

High-resolution SEM observations showed that K-feldspar albitization in the Qiongzhusi Formation samples is common, and five types of related textures have developed.

(1) Microcrystal albite replacement. This texture is a type of albitization that has not been reported and is less developed. This texture is developed in the sample from Majinzi that underwent dissolution and contains no calcite or dolomite. Therefore, it is preliminarily believed that the dissolution resulted in the loss of plagioclase early in the burial process. Thus, we provisionally regarded this texture as the result of K-feldspar albitization. In this texture, parent minerals (probably K-feldspars) are replaced by several albite microcrystals of various sizes, ranging from  $<1\ \mu\text{m}$  to more than  $10\ \mu\text{m}$  (Figure 5e–h). The single albite microcrystal is clean and anhedral and usually lacks authigenic smooth crystal surfaces and intragranular pores. Anhedral albite microcrystals in this texture usually forms mosaic textures. Pore fillings in the intercrystalline pores are common in this texture, but no K-feldspar relicts are found (Figure 5e–h). Semi-quantitative analysis by EDS confirms that the fillers are mainly illite and illite/montmorillonite mixed-layer minerals that have been contaminated by organic matter (Figure 9) and pyrite/limonite or apatite (Figure 5f–h). The albite microcrystals are small in size when the intercrystalline pores are filled with clay minerals (Figure 5e).



**Figure 9.** Enlarged view of the pore filling in Figure 5e. (a) Most of the fillings are illite and illite/montmorillonite mixed-layer minerals that have been contaminated by organic matter and mixed minerals of pyrite and limonite; (b) energy spectrum of spot 1 in (a), where the area is illite; and (c) energy spectrum of spot 2 in (a), where the area is illite/montmorillonite mixed-layer minerals.

(2) Irregular massive replacement. In this texture, albitization occurs along the margins, cleavage planes, or microcracks of K-feldspar grains (Figure 10). This texture is common in the study area and has been reported in mudstones [13]. Albitization is known to occur preferentially along cleavage surfaces or microcracks in K-feldspars [10,12,13,15]. However, if no cleavages or microcracks occurred in the K-feldspars (common in mudstones), then albitization would occur along the grain margins. Once the grain margin is completely albitized, further albitization of the K-feldspar would be difficult because the margin of the grain would be composed of stable albite [15].

(3) Complete replacement (pseudomorphic replacement). The complete albitization of K-feldspar in sandstones has been reported [9,10] and is very common in samples of the Qiongzhusi Formation from the study area. K-feldspar remnants and micropores are often found in this texture (Figure 11), indicating its secondary origin by replacement. In addition, small numbers of pyrite crystals and micropores with a certain trend can sometimes be observed in completely albitized particles. Connecting these pyrites and micropores, the whole particle seems to be divided into several albite crystals (Figure 11b), which may suggest that the pseudomorphic replacement albite is composed of several albite crystals with the same optical orientation. Saigal et al. (1988) also proposed that the pseudomorphic replacement of K-feldspars in sandstone formed through the merging of many albite crystals growing in the same

direction [10]. The difference between this structure and the microcrystal albite replacement texture is that replacement albite in this texture has been completely merged (possibly showing uniform extinction under an optical microscope) and often has K-feldspar remnants and micropores, while it does not in the microcrystal albite replacement texture.

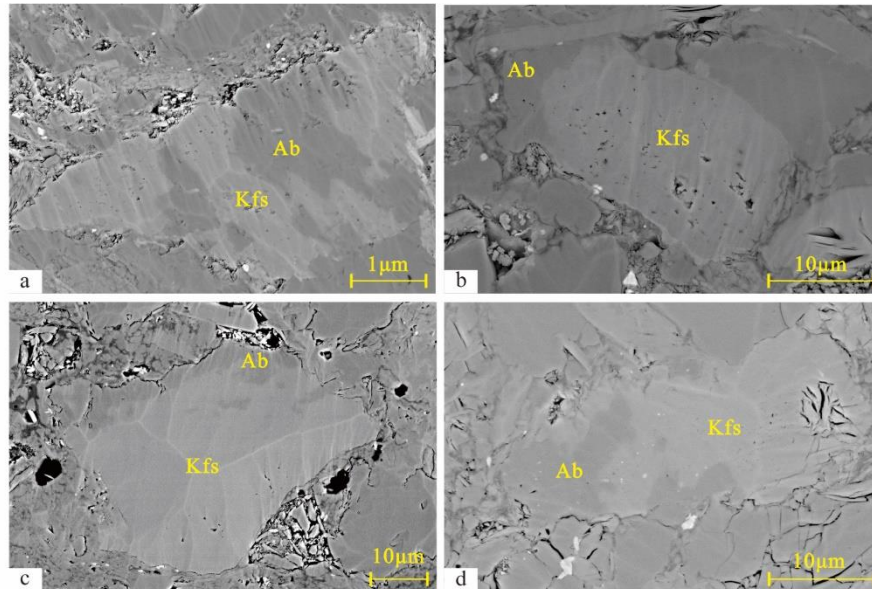


**Figure 10.** Irregular blocky replacement of K-feldspar from Majinzi. (a) Albitization of K-feldspar along cleavages or microcracks; and (b–d) albitization of K-feldspar along grain margins. Ab = albite, Kfs = K-feldspar.

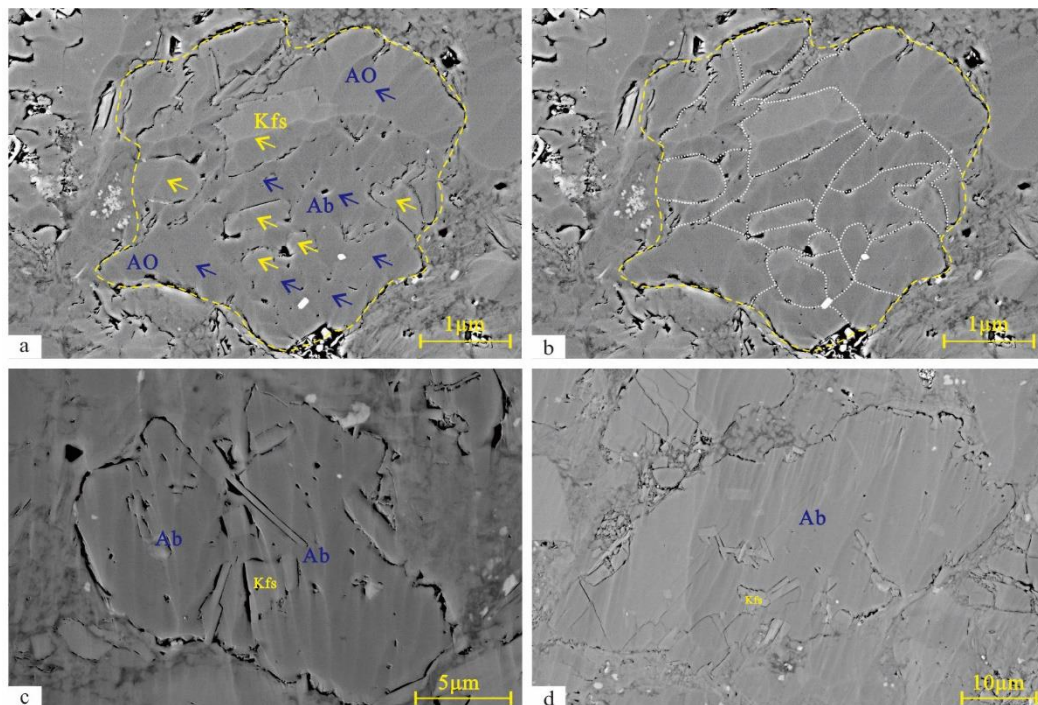


**Figure 11.** Complete replacement (pseudomorphic replacement) of K-feldspars. Note that K-feldspar remnants and micropores can be seen in the albitized K-feldspars (a,c,d), and the albitized K-feldspar in (a) seems to be composed of few K-feldspar remnants and several replacement albite (b); albite overgrowth is also obvious in (a). Ab and blue arrow = albite, AO = albite overgrowth, Kfs and yellow arrow = K-feldspar.

(4) Albite overgrowth (on the replacement albite grain). This texture has been reported in sandstones [10] and is very common in the studied samples of the Qiongzhusi Formation. The albite in this texture precipitates from pore water. Therefore, it is usually clean and free of inclusions [10,15]. The overgrowth albite in sandstone is mostly euhedral [10], but it is anhedral in samples of the Qiongzhusi Formation in the study area (Figure 11a), which may be related to the limited pore space for the growth of albite in fine-grained rocks (in sandstones, sufficient space is usually provided for albite growth, which results in coarser and euhedral albite. However, in fine-grained rocks, insufficient space is provided, which results in finer and anhedral albite).

(5) Albite pore filling. This texture has not been reported in fine-grained rocks and can be found in samples from Majinzi that contain no carbonate minerals (thus, we provisionally regarded this texture as the result of K-feldspar albitization). In this texture, the diagenetic anhedral albite that filled the matrix pores is clean, free of inclusions and pores, and usually less than 2.5  $\mu\text{m}$  in diameter (Figure 12). The pore-filling albite in sandstone are generally coarser, with platy, anhedral, or semi-anhedral shapes [9]. The differences in the pore-filling albite between sandstone and fine-grained rocks are also related to the limited pore space for albite growth.

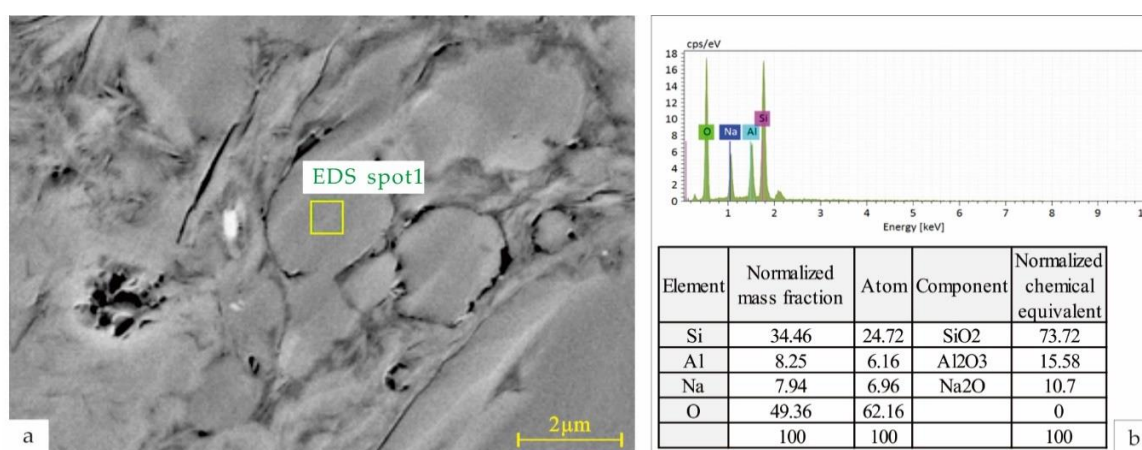


**Figure 12.** Albite pore filling. (a) Authigenic albite in a matrix pore; and (b) energy spectrum of EDS spot 1 in (a).

## 5. Discussion

### 5.1. Diagenetic Origin of the Albitization of K-Feldspar

Previous studies have shown that the albitization of K-feldspar is a common diagenetic process, and evidence suggesting its diagenetic origin has been proposed [9,10,12,13,15], which includes K-feldspar remnants in replacement albite, numerous fluid inclusions developed in replacement albite, a lack of cathodoluminescence of the replacement albite, the chemical purity of the overgrowth and replacement albite, the absence of albitization in the early carbonate-cemented rocks, etc. In this study, evidence of the diagenetic origin of the albitization of K-feldspar is as follows.

(1) Mosaic texture in the microcrystal albite replacement texture. In the microcrystal albite replacement texture, albite microcrystals are anhedral and form mosaic structures. Sometimes, one or more euhedral apatite crystals are engulfed in and closely surrounded by anhedral albite in the replacement albite microcrystals (Figure 5g). This suggests that euhedral apatite crystals formed prior to the formation of albite crystals and that the growth of minor albite occurred during diagenesis; that is, the replacement occurred during burial diagenesis.

(2) Albite overgrowth and albite pore filling (cementation). Albite overgrowth and albite pore filling are common phenomena in the study area. Albite formed by overgrowth and precipitation in pores are authigenic minerals during diagenesis, which is direct evidence of their diagenetic origin.

(3) Continuous development of complete replacement texture. In some complete replacement textures, continuous development of the albitization texture can be observed, in which several albite crystals gradually merge into one albite and relict K-feldspar are often found in the replacement albite grain (Figure 11b). This continuous development of the albitization texture indicates that albitization occurred during diagenesis. It is also possible that some complete replacement albite originated from source rocks.

(4) Differences in the texture of albitized K-feldspar between the samples studied and the overlying fine-grained rocks (poor in organic matter). In the overlying fine-grained rocks, the microcrystal albite replacement texture is absent (Figure 13). If albitization occurred in the source rocks, the same structures should be found in the adjacent rocks. Thus, a different albitization did take place in the adjacent layers during diagenesis.

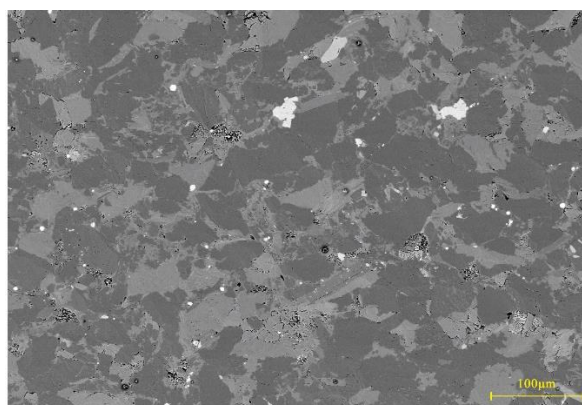


**Figure 13.** Backscattered electron image of overlying fine-grained rocks (dark gray grains are quartz or albite; light gray grains are K-feldspar and carbonate minerals; and bright white grains are pyrite. Note that no microcrystal albite replacement texture is found in the whole image).

## 5.2. Origin of Microcrystal Albite Replacement

For this structure, there is no direct evidence of its origin from K-feldspar. Therefore, we can only indirectly infer that it may originate from K-feldspar. In this structure, there is evidence that the parent minerals (probably K-feldspar) had undergone dissolution before albitization. In the case of a K-feldspar grain lacking intragranular dissolved pores, a common albitization pathway is for a large amount of microcrystalline albite to initially form in isolation in different positions in the K-feldspar grain, and then albite crystals grow and merge gradually as the albitization proceeds [9,10]. The combination of these albite crystals indicates that the albite crystals newly formed by this pathway have the same optical direction. Under an optical microscope, uniform extinction is observed for the replacement albite formed in this way [10,12,17]. However, when a considerable number of intragranular pores are developed in the K-feldspar grain because of dissolution, some albite would precipitate in the solution pores during albitization. Accordingly, the newly formed albite crystals cannot easily grow in a uniform optical direction and will inevitably lead to the formation of a mosaic structure with continued albitization, because some albite crystals cannot merge for their different optical directions. For example, Saigal et al. (1988) observed that an interlocking structure developed in a possibly dissolved K-feldspar in a relatively earlier stage of albitization in his study. Because K-feldspar albitization is a volume-reducing reaction [11], irregular intergranular pores often form between the replacement albite crystals (Figure 5g,h). This texture did not develop in the samples of overlying organic-poor fine-grained rocks, which may indicate that the diagenesis processes that the overlying samples have undergone differed from those of the bottom samples.

According to the positional relationship between diagenetic minerals and as discussed above, the formation of this structure in the study area has undergone the following diagenetic sequence: dissolution and intragranular dissolved pores forming in the early eogenesis (Figure 14b) → filling of

intragranular dissolved pores by authigenic euhedral apatite and matrix (montmorillonite perhaps) under compaction (Figure 14c) → albitization (Figure 14d–f) → filling of intragranular pores by anhedral pyrite (Figure 14g) → filling of residual intragranular pores, if any, by liquid hydrocarbon expelled by the matured kerogen (Figure 14h).

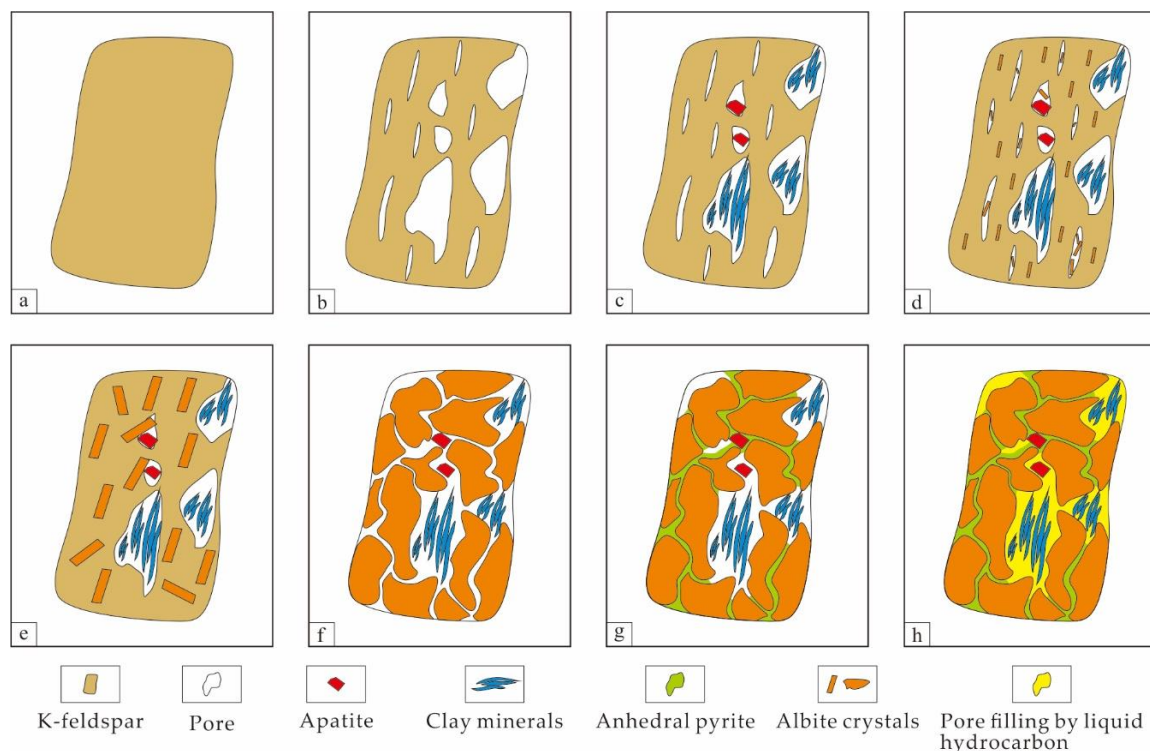


**Figure 14.** Conception map of the formation of microcrystal albitite replacement texture of the albitized K-feldspar in the Qiongzhusi Formation without considering mechanical compaction. (a) Original K-feldspar particle; (b) partial dissolution of the K-feldspar particle; (c) filling of intragranular dissolved pores by authigenic euhedral apatite and matrix under compaction; (d–f) albitization of the K-feldspar; (g) filling of intragranular pores by anhedral pyrite; and (h) filling of residual intragranular pores by liquid hydrocarbon.

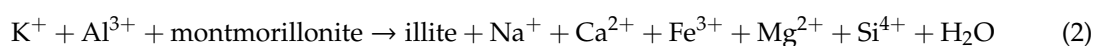
### 5.3. Coupled Illitization of Smectite/Kaolinite and Albitization of K-Feldspar in Fine-Grained Rocks and Its Implication

The reaction of K-feldspar albitization may be described as below [9–11]:

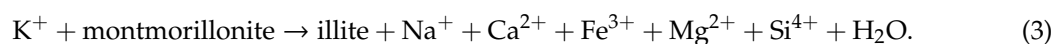


In the above reaction, K-feldspar loses  $\text{K}^+$ , gains  $\text{Na}^+$ , and transforms into albite. Saigal et al. (1988) found that the albitization of K-feldspar during burial started at a temperature of 65 °C and that the maximum reaction temperature exceeded 105 °C [10].

When the formation temperature exceeds approximately 50 °C and  $\text{K}^+$  is supplied in the formation, the alteration of smectite to illite occurs [16,30], which can be described as follows [30]:



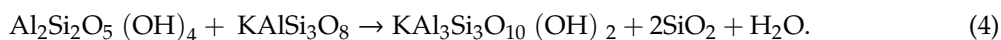
or



According to Equations (2) and (3), the alteration of smectite to illite would consume  $\text{K}^+$  and release  $\text{Na}^+$ ,  $\text{Ca}^{2+}$ ,  $\text{Fe}^{3+}$ ,  $\text{Mg}^{2+}$ , and  $\text{Si}^{4+}$ , while  $\text{Si}^{4+}$  would precipitate in the form of quartz. These reactions

are mainly driven by depth/temperature, and their reaction temperatures range from 50 °C to over 175 °C (but the reactions mainly occur at 60–100 °C) [16,30,42].

In addition, the alteration of kaolinite to illite at higher temperatures (in excess of 120–130 °C) would consume  $K^+$  [31,32]:



In fine-grained rocks containing the above minerals, Reaction (1) would theoretically couple with Reactions (2–4), providing an effective K-sinking mechanism for Reaction (1) to remove  $K^+$  from pore water to ensure that Reaction (1) continues during diagenesis. Previous studies suggested that this coupling did work during diagenesis [10,16,30,42,43]. For example, Perry and Hower (1970) and Hower et al. (1976) proposed that the main source of potassium for the conversion of smectite to illite was the decomposition of K-feldspar [16,43], and several studies have suggested that the reaction window of Reaction (1) overlaps with those of Reactions (2–4), which can also be regarded as evidence for the coupling reactions [10,16,30,42]. In the Qiongzhusi Formation, the effect of Reaction (4) on K-feldspar albitization may be limited because the temperature required for Reaction (4) is likely to be higher than that of the oil window. Since the albitization of K-feldspar was proposed [12], the coupling of K-feldspar albitization and smectite/kaolinite illitization has been widely used in diagenetic studies [3,9,10,17]. For example, when Chowdhury and Noble (1993) studied the feldspar albitization of sandstones in the Albert Formation, they observed that there was no trend in the volume percentage of albitization of K-feldspar with increasing burial depth in the Albert Formation, and that the albitization of K-feldspar stopped at low temperatures [9]. They suggested that the cessation of albitization at low temperatures was related to the failure to remove the  $K^+$  released by Reaction (1) from pore water [9].

Fine-grained rocks usually contain considerable amounts of clay minerals, feldspar including K-feldspar, and other minerals. Therefore, strong coupling of the above reactions would presumably occur during the diagenesis of fine-grained rocks and have an effect on the albitization of K-feldspar. For some sandstones, due to their low clay mineral content, there might be a lack of an effective K-sinking mechanism in the diagenetic processes, which would lead to a lower degree of albitization of K-feldspar. For example, Saigal et al. (1988) estimated that only 7–10% of the K-feldspar in sandstones from different formations shows evidence of albitization [10], whereas Chowdhury and Noble (1993) found that the volume percentage of replacement albite in the detrital K-feldspars of sandstones ranges from 21% to 50% (mean: 33%) and showed no systematic change with burial depth [9]. However, for fine-grained rocks, due to the existence of an effective  $K^+$ -sinking mechanism, the degree of albitization should be relatively high. According to Milliken (1992), approximately 56–68% of K-feldspar has been albitized, which is higher than the rate for sandstones reported by Saigal et al. (1988) and Chowdhury and Noble (1993) [9,10]. In this study, it is preliminarily believed that none or very little diagenetic albite originated from plagioclase for the samples from Majinzi. If all albite originated from K-feldspar albitization for these samples, the degree of albitization of K-feldspar would be between 68% and 90%, with an average of 83% (assuming that all the plagioclase in the samples is albite). However, as part of the albite may be derived from mother rocks, the actual degree of albitization should be lower than the above value. Unfortunately, we are not sure how much albite comes from mother rocks; therefore, the exact value of the degree cannot be determined. However, we believe that the degree of albitization of K-feldspar in fine-grained rocks should be high because of the K-sinking mechanism during diagenesis.

#### 5.4. Mechanisms of K-Feldspar Albitization

Previous studies have suggested that K-feldspar albitization proceeds through a dissolution/precipitation mechanism [14]. In the complete replacement texture of the albitized K-feldspar, some replacement albite grains are irregular in appearance (Figure 11a,c), which may be caused

by the collapse of grains under compaction as a result of the reduced grain volume because some dissolved material of the K-feldspar precipitated in adjacent pores or as overgrowth on albite grains. In addition, there are narrow gaps between the replacement albite and K-feldspar in some partially albitized K-feldspar (Figure 15a), which indicate that the albitization of K-feldspar proceeds through dissolution/precipitation mechanism. Texture evidence and previous studies [39] suggest that the albitization of K-feldspar in the Qiongzhusi Formation mainly occurred before the oil window, and Figure 5g shows that euhedral apatite crystals predate albitization. However, the earliest time of albitization of K-feldspar is also unknown in the Qiongzhusi Formation. In Chowdhury and Noble's (1993) study, the earliest time of albitization of K-feldspar was considered to be shortly after burial [9]. In the Qiongzhusi Formation, we occasionally find non-albitized K-feldspar (Figure 15b). The difference in albitization between K-feldspar grains may be caused by their different compositions (the purer the composition of a K-feldspar grain is, the less likely it is to be albitized) [14]. In conclusion, the following K-feldspar albitization process is proposed for the Qiongzhusi Formation: The albitization of K-feldspar started at shallow burial and continued to the oil window through the dissolution/precipitation mechanism. The composition of K-feldspar grains and the illitization of clay minerals before the oil window influence the process. During the albitization of K-feldspar, some dissolved material precipitated in situ, forming replacement albite, while the others precipitated in adjacent pores or as overgrowth on albite. When the dissolved material was mainly deposited in situ and K-feldspar lacked dissolved pores, the irregular massive replacement texture or the complete replacement texture would be formed. Alternatively, if numerous dissolved pores were developed in the K-feldspar grains, the microcrystal albite replacement structure would be formed. The Na required for the albitization mainly came from pore water; it is not clear whether there are other Na sources.

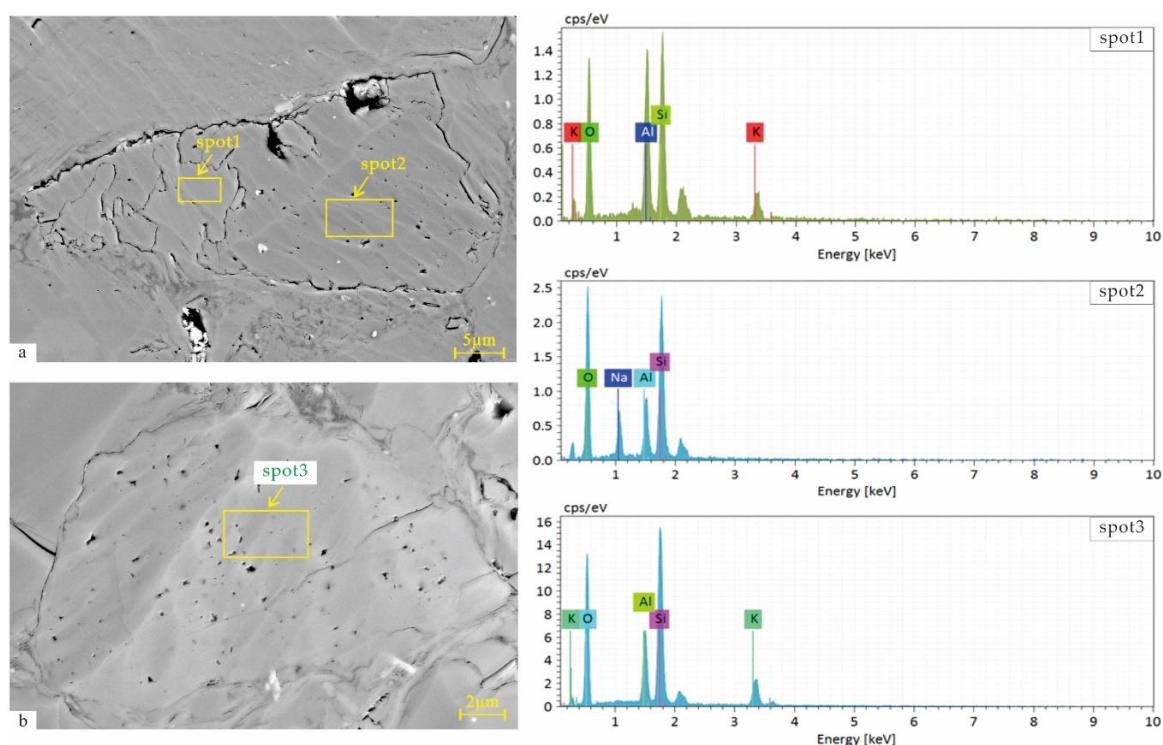


**Figure 15.** (a) A partially albitized K-feldspar and (b) a non-albitized K-feldspar. Energy spectrums in the yellow box in (a) and (b) are placed to the right.

### 5.5. Differences between Fine-Grained Rocks and Sandstones in the Albitization of K-Feldspar

Numerous studies on sandstones [2,6,9,10,12,13,17] and a few studies on mudstones [14,15] have suggested that the diagenetic albitization of K-feldspar is a common process in both rocks.

However, there are differences between sandstones and fine-grained rocks in the albitization of K-feldspar [9,10,12–15,17].

In sandstones, the main textures of albitized K-feldspar that have been reported are numerous tiny euhedral albite crystals replacement, chessboard irregular albitization, albitization along grain margins, albitization along cleavage planes and microfractures, complete albitization, albite overgrowth, and pore fillings or albite cements [9,10,12,17], whereas in mudstones, only a few types of textures of albitized K-feldspar have been reported, including albitization along grain margins, cleavage planes, or microfractures [14]. In the Qiongzhusi Formation, five types of textures were observed, which are similar to those of sandstones [9,10,12,17]. With respect to the degree of albitization of K-feldspar, limited data have been provided by previous researchers. From these limited studies, it can be found that the degree of albitization of K-feldspar in sandstones can be high or low, which is related to specific geological conditions [9,10,14,44]. However, for fine-grained rocks, because of the above coupling, the degree of albitization of K-feldspar should usually be high [14]. Milliken (1992) questioned the usefulness of mudstones in provenance analysis because detrital feldspar can be destroyed by albitization to varying degrees [14]. As we predicted, a large amount of K-feldspar has been albitized from SEM observation in this study. Thus, although the exact degree of albitization of K-feldspar has not been obtained in this study, a similar suggestion is made for silt-rich fine-grained rocks that have undergone mesogenesis. It can be seen that for the Qiongzhusi Formation, with respect to the texture of albitized K-feldspar, they are similar to those of sandstones; in contrast, regarding the degree of albitization of K-feldspar, they might be similar to that of mudstones. The differences in rock structure and mineral assemblage among the three types of rocks might account for these differences. In rock structure, silt-rich fine-grained rocks of the Qiongzhusi Formation, which are coarser in grain size than mudstones and similar to sandstones, are mainly supported by detrital grains. The grain-supported structure means that the rocks can retain more pore space and a higher permeability than mudstones under the same overlying pressure during compaction, which is helpful for albitization [10,14] and may result in similar textures with sandstones. In the mineral assemblage, silt-rich fine-grained rocks of the Qiongzhusi Formation are rich in clay mineral content, which is similar to mudstones and would result in a relatively high extent of albitization of K-feldspar because of the above coupling reactions.

Dissolution/precipitation is the common mechanism of albitization of K-feldspar in sandstones and fine-grained rocks [14,17]. However, in terms of the time and stage of K-feldspar albitization, sandstones seem to be more dependent on the precipitation of K from pore water or transportation of K out of the formation rather than temperature/burial depth [9,10,17]. Affected by this, the time of albitization between sandstones varies greatly, sometimes showing multi-stage albitization [9,10]. For example, Chowdhury and Noble (1993) found that the K-feldspar albitization process in the Albert Formation sandstones stopped at low temperatures because the K released by K-feldspar was not removed from the pore water. However, Saigal et al. (1988) reported that K-feldspar albitization proceeded at temperatures over 95 °C in their study on sandstones. Because of the K-sinking mechanism, albitization in fine-grained rocks may occur mostly in the transformation zone of clay minerals to illite. In source rocks, because of the hydrocarbon generation, especially during the oil window, K-feldspar albitization process would be inhibited.

## 5.6. The Effect of the Albitization of K-Feldspar on Fine-Grained Reservoirs

### 5.6.1. The Effect of the Albitization of K-Feldspar on the Porosity of Fine-Grained Rocks

Reaction (1) shows that 1 mol of albite replaces 1 mol of K-feldspar. Due to the different molar volumes (the molar volume of K-feldspar is 109.1 cm<sup>3</sup>/mol, and that of albite is 100.2 cm<sup>3</sup>/mol), an approximately 8% volume reduction can be generated after the albitization of K-feldspar [11,45]. According to FE-SEM images, the pores related to the albitization of K-feldspar are mainly intercrystalline pores in the microcrystal albite replacement texture (Figure 5d–g) and intragranular pores in completely replaced albite (pseudomorphic replacement) (Figure 11). Intercrystalline pores

in microcrystal albite replacement texture are usually filled by clay minerals, pyrite, and/or apatite. The intragranular pores in completely replaced albite mainly hold fluid inclusions [10], which are not connected in three-dimensional space [11]; therefore, they are ineffective pores. Pores might be formed between albitized grains and matrix during the albitization of K-feldspar. However, due to the compaction and growth of authigenic minerals in pores, most of these pores have been filled in and/or have disappeared. Milliken (1992) also found that intragranular pores in feldspars are scarce in Frio mudrocks due to compaction [14]. Therefore, in theory, K-feldspar albitization would increase porosity, although, in general, most of these newly formed pores have been offset by other diagenetic processes (such as compaction and cementation) or have become isolated pores.

#### 5.6.2. The Effect of the Albitization of K-feldspar on Shale Gas Reservoir Quality

Industrial gas flow has been obtained from organic- and silt-rich fine-grained rocks of the Qiongzhusi Formation in adjacent areas [19]. This success indicates that organic- and silt-rich fine-grained rocks can also be potential shale gas reservoirs. K-feldspar albitization is one of the most common diagenetic processes in the Qiongzhusi Formation and provides  $K^+$  for smectite/kaolinite illitization, which releases large amounts of  $SiO_2$  [16,30]. Most of this  $SiO_2$  is retained in the formation in the form of quartz overgrowths and cements in microcrystals, which are very helpful both for increasing the brittleness of shales and developing shale gas [2,4,7,8]. In addition, from our observations, a part of the albite newly formed during diagenesis is directly filled into the pores as cements or precipitated in the form of albite overgrowth, which is also conducive to increasing the brittleness of the rocks. Therefore, in general, K-feldspar albitization is beneficial for fine-grained rocks to improve their brittleness and quality as a shale gas reservoir.

### 6. Conclusions

(1) The albitization of K-feldspar is common in organic- and silt-rich fine-grained rocks in the Qiongzhusi Formation. The mosaic structure in the microcrystal albite replacement texture, albite overgrowth, and albite cements, the continuous development of complete replacement texture, and the difference in textures of albitized K-feldspar between studied rocks and overlying organic-poor fine-grained rocks can provide evidence for the diagenetic origin of the albitization of K-feldspar.

(2) The albitization of K-feldspar in the Qiongzhusi Formation started at shallow burial depths and continued to the oil window through the dissolution/precipitation mechanism. Five types of textures of albitized K-feldspar have developed: microcrystal albite replacement, irregular blocky replacement along the margins, cleavage planes or microcracks of K-feldspars, complete replacement (pseudomorphic replacement), albite overgrowth, and albite pore filling. Dissolved pores in the K-feldspar grains may have an impact on the formation of the textures.

(3) Organic- and silt-rich fine-grained rocks differ from sandstones and mudstones in their rock structure and mineral assemblage, which results in the differences in albitization of K-feldspar. Regarding the textures of albitized K-feldspar, the silt-rich fine-grained rocks of the Qiongzhusi Formation are similar to those of sandstones, but quite different from those of mudstones. With respect to the degree of albitization of K-feldspar, in the silt-rich fine-grained rocks of the Qiongzhusi Formation it is usually as high as in mudstones, whereas for sandstones, the value can be high or low depending on the geological conditions. Therefore, in the provenance analysis using feldspar, fine-grained rocks, especially those that have undergone mesogenesis, should be treated with caution.

(4) In theory, K-feldspar albitization would increase the porosity of rocks, although from our observations, most of the related secondary pores are cancelled out or become isolated pores by other diagenetic processes (compaction, cementation, etc.) in the studied samples. However, albitization is conducive to increasing the brittleness of the rock. Therefore, in general, K-feldspar albitization is beneficial to improving the quality of fine-grained rocks as a shale gas reservoir.

(5) It should be emphasized that our study is based on organic- and silt-rich fine-grained rocks that have undergone mesogenesis. The findings in this paper cannot be extended to all fine-grained rocks,

such as mudstones, because the differences in rock structure and original mineral assemblage among different fine-grained rocks will likely have an effect on the albitization of K-feldspar. Furthermore, we cannot rule out the possibility that some albite or partially albitized K-feldspar may be inherited from source rocks, which would affect the estimation of the extent to which the K-feldspar has albitized in the rocks.

**Author Contributions:** Conceptualization, H.M., T.Z. and Y.L.; methodology, H.M. and S.Z.; validation, H.M., J.L., D.L. and J.W.; formal analysis, D.L. and J.W.; investigation, H.M., J.L. and S.Z.; resources, T.Z. and Y.L.; data curation, H.M., and J.L.; writing—original draft preparation, H.M.; writing—review and editing, H.M., D.L. and J.W.; visualization, S.Z.; supervision, H.M., T.Z. and Y.L.; project administration, S.Z., J.L. and D.L.; funding acquisition, T.Z. and Y.L.

**Funding:** This research was funded by the National Natural Science Foundation of China (grant number 41772150), National Science and Technology Major Project of China (grant number 2017ZX05063002-009), Sichuan Province's Key Project of Research and Development (grant number 18ZDYF0884), and the Sichuan Province Science and Technology Plan Project (grant number 2019YJ0468).

**Conflicts of Interest:** The authors declare no conflict of interest.

## References

- Picard, M.D. Classification of Fine-grained Sedimentary Rocks. *J. Sediment. Res.* **1971**, *41*, 179–195.
- Peltonen, C.; Marcussen, Ø.; Bjørlykke, K.; Jahren, J. Clay mineral diagenesis and quartz cementation in mudstones: The effects of smectite to illite reaction on rock properties. *Mar. Pet. Geol.* **2009**, *26*, 887–898. [[CrossRef](#)]
- Day-Stirrat, R.J.; Milliken, K.L.; Dutton, S.P.; Loucks, R.G.; Hillier, S.; Aplin, A.C.; Schleicher, A.M. Open-system chemical behavior in deep Wilcox Group mudstones, Texas Gulf Coast, USA. *Mar. Pet. Geol.* **2010**, *27*, 1184–1818. [[CrossRef](#)]
- Thyberg, B.; Jahren, J. Quartz cementation in mudstones: Sheet-like quartz cement from clay mineral reactions during burial. *Petrol. Geosci.* **2011**, *17*, 53–63. [[CrossRef](#)]
- Taylor, K.G.; Macquaker, J.H.S. Diagenetic alterations in a silt- and clay-rich mudstone succession: An example from the upper Cretaceous Mancos shale of Utah, USA. *Clay Min.* **2014**, *49*, 213–227. [[CrossRef](#)]
- Dowey, P.J.; Taylor, K.G. Extensive authigenic quartz overgrowths in the gas-bearing Haynesville-Bossier Shale, USA. *Sediment. Geol.* **2017**, *356*, 15–25. [[CrossRef](#)]
- Milliken, K.L.; Olson, T. Silica diagenesis, porosity evolution, and mechanical behavior in siliceous mudstones, Mowry shale (Cretaceous), Rocky Mountains, U.S.A. *J. Sediment. Res.* **2017**, *87*, 366–387. [[CrossRef](#)]
- Delle Piane, C.; Almqvist, B.S.G.; Macrae, C.M.; Torpy, A.; Mory, A.J.; Dewhurst, D.N. Texture and diagenesis of Ordovician shale from the canning basin, Western Australia: Implications for elastic anisotropy and geomechanical properties. *Mar. Pet. Geol.* **2015**, *59*, 56–71. [[CrossRef](#)]
- Chowdhury, A.H.; Noble, J.P.A. Feldspar albitization and feldspar cementation in the Albert formation reservoir sandstones, New Brunswick, Canada. *Mar. Pet. Geol.* **1993**, *10*, 394–402. [[CrossRef](#)]
- Saigal, G.C.; Morad, S.; Bjørlykke, K.; Egeberg, P.K.; Aagaard, P. Diagenetic albitization of detrital k-feldspar in jurassic, lower cretaceous, and tertiary clastic reservoir rocks from offshore Norway, I. textures and origin. *J. Sediment. Res.* **1988**, *58*, 1003–1013.
- Norberg, N.; Neusser, G.; Wirth, R.; Harlov, D. Microstructural evolution during experimental albitization of k-rich alkali feldspar. *Contrib. Mineral. Petrol.* **2011**, *162*, 531–546. [[CrossRef](#)]
- Middleton, G.V. Albite of secondary origin in charny sandstones Quebec. *J. Sediment. Res.* **1972**, *42*, 341–349. [[CrossRef](#)]
- Walker, T.R. Diagenetic albitization of potassium feldspar in arkosic sandstones. *J. Sediment. Res.* **1984**, *54*, 3–16.
- Milliken, K.L. Chemical behavior of detrital feldspars in mudrocks versus sandstones, Frio formation (Oligocene), South Texas. *J. Sediment. Res.* **1992**, *62*, 790–801.
- Lee, J.I.; Lee, Y.I. Feldspar albitization in Cretaceous non-marine mudrocks, Gyeongsang Basin, Korea. *Sedimentology* **1998**, *45*, 745–754. [[CrossRef](#)]
- Hower, J.; Eslinger, E.V.; Hower, M.E.; Perry, E.A. Mechanism of burial metamorphism of argillaceous sediment: 1. mineralogical and chemical evidence. *Geol. Soc. Am. Bull.* **1976**, *87*, 725–737. [[CrossRef](#)]

17. Morad, S. Albitization of K-feldspar grains in Proterozoic arkoses and greywackes from southern Sweden. *N. Jahrb. Mineral. Monatsh* **1986**, *4*, 145–156.
18. González-Acebrón, L.; Arribas, J.; Mas, R. Role of sandstone provenance in the diagenetic albitization of feldspars: A case study of the Jurassic Tera Group sandstones (Camerós Basin, NE Spain). *Sediment. Geol.* **2010**, *229*, 53–63. [[CrossRef](#)]
19. Zeng, Y.-J.; Chen, Z.; Bian, X.-B. Breakthrough in staged fracturing technology for deep shale gas reservoirs in SE Sichuan Basin and its implications. *Nat. Gas Ind.* **2016**, *36*, 61–67. [[CrossRef](#)]
20. Zhu, C.-Q.; Rao, S.; Yuan, Y.-S.; Wang, Q.; Qiu, N.-S.; Hu, S.-B. Thermal evolution of the main Paleozoic shale rocks in the southeastern Sichuan basin. *J. China Coal Soc.* **2013**, *38*, 834–839.
21. Li, J.; Wang, Y.-F.; Ma, W.; Wang, D.-L.; Ma, C.-H.; Li, Z.-S. Evaluation on occluded hydrocarbon in deep-ultra deep ancient source. *Nat. Gas Ind.* **2015**, *35*, 9–15.
22. Wei, G.-Q.; Yang, W.; Xie, W.-R.; Jin, H.; Su, N.; Sun, A.; Shen, J.-H.; Hao, C.-G. Accumulation modes and exploration domains of Sinian-Cambrian natural gas in Sichuan Basin. *Acta Petrol. Sin.* **2018**, *39*, 1317–1327.
23. Zhang, A.-Y.; Wu, D.-M.; Guo, L.-N.; Wang, Y.-L. *Geochemistry of Marine Black Shale Formation and its Metallogenic Implication*; Science Press: Beijing, China, 1987; pp. 13–30.
24. Wu, S.-J.; Wei, G.-Q.; Yang, W.; Xie, W.-R.; Zeng, F.-Y. Tongwan Movement and its geologic significances in Sichuan Basin. *Nat. Gas Geosci.* **2016**, *27*, 60–70.
25. Liu, Z.-B.; Gao, B.; Zhang, Y.-Y.; Du, W.; Feng, D.-J.; Nie, H.-K. Types and distribution of the shale sedimentary facies of the Lower Cambrian in Upper Yangtze area, South China. *Petrol. Explor. Dev.* **2017**, *44*, 21–31. [[CrossRef](#)]
26. Liu, B.-J.; Xu, X.-S. *Lithofacies Palaeogeography Atlas of Southern China (Sinian-Triassic)*; Science Press: Beijing, China, 1994; pp. 42–43.
27. Wang, P.-W.; Zhang, L.; Zou, C.; Song, H.-Q.; Chen, Z.-L.; Wang, G.-C.; Li, J.-J.; Li, Q.-F. Exploration direction of highly mature shale gas from Qiongzhusi Formation in Zhenxiong- Hezhang area of Southwest China. *J. Chengdu Univ. Technol.* **2015**, *42*, 530–538.
28. Chalmers, G.R.L.; Bustin, R.M. Lower Cretaceous gas shales in northeastern British Columbia, part I: Geological controls on methane sorption capacity. *Bull. Can. Petroleum Geol.* **2008**, *56*, 1–21. [[CrossRef](#)]
29. China National Energy Administration. *Analysis Method for Clay Minerals and Ordinary Non- Clay Minerals in Sedimentary Rocks by the X-Ray Diffraction*; Petroleum Industry Press: Beijing, China, 2018; pp. 1–47.
30. Boles, J.R.; Franks, S.G. Clay diagenesis in Wilcox sandstones of southwest Texas: Implications of smectite diagenesis on sandstone cementation. *J. Sediment. Res.* **1979**, *49*, 55–70.
31. Bjørlykke, K.; Aagaard, P.; Dypvik, H.; Hastings, D.S.; Harper, A.S. Diagenesis and reservoir properties of Jurassic sandstones from the Haltenbanken area, offshore mid-Norway. In *Habitat of Hydrocarbons on the Norwegian Continental Shelf*; Spencer, A.M., Ed.; Norwegian Petroleum Society (Graham & Trotman): Oslo, Norway, 1986; pp. 275–286.
32. Chuhan, F.A.; Bjørlykke, K.; Lowrey, C.J. Closed-System Burial Diagenesis in Reservoir Sandstones: Examples from the Garn Formation at Haltenbanken Area, Offshore Mid-Norway. *J. Sediment. Res.* **2001**, *71*, 15–26. [[CrossRef](#)]
33. Milliken, K.L.; Ergene, S.M.; Ozkan, A. Quartz types, authigenic and detrital, in the upper cretaceous eagle ford formation, south Texas, USA. *Sediment. Geol.* **2016**, *339*, 273–288. [[CrossRef](#)]
34. Zhao, S.-Z.; Li, Y.; Min, H.-J.; Wang, T.; Nie, Z.; Zhao, Z.-Z.; Qi, J.-Z.; Wang, J.-C.; Wu, J.-P. Development of Upwelling during the Sedimentary Period of the Organic-Rich Shales in the Wufeng and Longmaxi Formations of the Upper Yangtze Region and Its Impact on Organic Matter Enrichment. *J. Mar. Sci. Eng.* **2019**, *7*, 99. [[CrossRef](#)]
35. Wilkin, R.T.; Barnes, H.L.; Brantley, S.L. The size distribution of framboidal pyrite in modern sediments: An indicator of redox conditions. *Geochim. Cosmochim. Acta* **1996**, *60*, 3897–3912. [[CrossRef](#)]
36. Wilkin, R.T.; Barnes, H.L. Formation processes of framboidal pyrite. *Geochim. Cosmochim. Acta* **1997**, *61*, 323–339. [[CrossRef](#)]
37. Bond, D.P.G.; Wignall, P.B. Pyrite framboid study of marine permian-triassic boundary sections: A complex anoxic event and its relationship to contemporaneous mass extinction. *Bull. Geol. Soc. Am.* **2010**, *122*, 1265–1279. [[CrossRef](#)]
38. Potter, P.E.; Maynard, J.M.; Depetris, P.J. *Mud and Mudstones*; Springer: Berlin, Germany, 2005; p. 150.

39. Worden, R.H.; Oxtoby, N.H.; Smalley, P.C. Can oil emplacement prevent quartz cementation in sandstones? *Petrol. Geosci.* **1998**, *4*, 129–137. [[CrossRef](#)]
40. Milliken, K.L. Late diagenesis and mass transfer in sandstone—Shale sequences. In *Treatise on Geochemistry*; Holland, H.D., Turekian, K.K., Eds.; Elsevier: Amsterdam, The Netherlands, 2003; pp. 159–190.
41. Bjørlykke, K.; Jahren, J. Open or closed geochemical systems during diagenesis in sedimentary basins: Constraints on mass transfer during diagenesis and the prediction of porosity in sandstone and carbonate reservoirs. *AAPG Bull.* **2012**, *96*, 2193–2214. [[CrossRef](#)]
42. Lynch, F.L.; Mack, L.E.; Land, L.S. Burial diagenesis of illite/smectite in shales and the origins of authigenic quartz and secondary porosity in sandstones. *Geochim. Cosmochim. Acta* **1997**, *61*, 1995–2006. [[CrossRef](#)]
43. Perry, E.; Hower, J. Burial diagenesis in gulf coast pelitic sediments. *Clay Clay Min.* **1970**, *18*, 165–177. [[CrossRef](#)]
44. Dutton, S.P.; Loucks, R.G. Diagenetic controls on evolution of porosity and permeability in lower Tertiary Wilcox sandstones from shallow to ultradeep (200–6700 m) burial, Gulf of Mexico basin, USA. *Mar. Pet. Geol.* **2010**, *27*, 69–81. [[CrossRef](#)]
45. Lin, C.-X.; Bai, Z.-H.; Zhang, Z.-R. *Thermodynamic Data Manual for Minerals and Related Compounds*; Science Press: Beijing, China, 1985; pp. 214–265.



© 2019 by the authors. Licensee MDPI, Basel, Switzerland. This article is an open access article distributed under the terms and conditions of the Creative Commons Attribution (CC BY) license (<http://creativecommons.org/licenses/by/4.0/>).